Available online at www.sciencedirect.com
SCIENCE DIRECT®
Electrochemistry Communications 5 (2003) 120–123
electrochemistry communications
www.elsevier.com/locate/elecom

3-D Microbatteries

Ryan W. Hart [a], Henry S. White [a,*], Bruce Dunn [b], Debra R. Rolison [c]

[a] Department of Chemistry, University of Utah, Salt Lake City, UT 84112, USA
[b] Department of Materials Science and Engineering, University of California, Los Angeles, Los Angeles, CA 90095, USA
[c] Surface Chemistry Branch, Code 6170, Naval Research Laboratory, Washington, DC 20375, USA

Received 15 November 2002; received in revised form 19 December 2002; accepted 19 December 2002

Abstract

Batteries based on three-dimensional (3-D) microstructures are shown to offer significant advantages (e.g., small areal footprint, short diffusion lengths) in comparison to thin film devices for powering microelectromechanical systems and miniaturized electronic devices. A key limitation in all 3-D periodic cell architectures is the inherent non-uniform current density. Finite-element simulations of the current and potential in several cathode/anode array configurations are presented to illustrate the difficulty in obtaining relatively uniform current densities in 3-D batteries based on periodic elements.

Keywords: Battery; Three-dimensional microbattery; Energy storage; Finite-element simulation; Current distribution.

1. Introduction

One of the recent themes to emerge from several high technology areas is the prospect of exploiting three-dimensional (3-D) structures. Among the areas where 3-D structures offer promising opportunities are photonic crystals for optical devices and components [1,2], optical data storage [3], magnetic data storage [4], chemical and biochemical sensors [5,6], 3-D lithographic microfabrication [7,8], and 3-D self-assembled structures [9,10].

The present paper considers the design of a 3-D battery, Fig. 1, and identifies several advantages and limitations that this configuration offers. One motivation for exploring such 3-D configurations is to develop portable power sources of millimeter dimensions that contain sufficient active material to power microelectromechanical systems (MEMS) devices and microelectronic circuits for extended periods of time. With 3-D structures, making the electrodes longer (i.e., increasing L in Fig. 1), rather than thicker leads to increased cell capacity while retaining the same areal footprint (i.e., square footage) on the surface of the device. In this way, energy density is not traded for power density.

Conventional batteries are 2-D cells with a parallel (or pseudo-parallel) arrangement of planar cathode and anode separated by an electrolyte. Our use of the terminology 3-D in the present context denotes cells comprising anodes and cathodes which have active surface areas exposed in three dimensions. The cylinder is the prototype electrode geometry considered here, although not necessarily the optimal geometry in constructing a microbattery (vide infra).

In order to maximize energy and power density, 3-D microbatteries will comprise a large number of closely spaced cathodes and anodes, such as the example shown in Fig. 1. (Note: the current collectors at the bases of the cathodes and anodes are not shown). While such a 3-D integrated design has yet to be realized, it is expected that the fabrication of 3-D electrode configurations will be based on exploiting current lithographic technology that can produce essentially any desired electrode pattern in any desired arrangement of electrodes. Clearly, the sizes and relative placement of the electrodes determine the performance of the device. Maximizing the number density (cm^{-2}) of cathodes and anodes, while minimizing the separation between them, increases both energy and power density. However, in contrast to a 2-D battery, in which a uniform current density is naturally obtained over the surfaces of the cathode and anode, the

* Corresponding author. Tel.: 1-801-585 6256; fax: +1-801-581 5720.
E-mail address: white@chemistry.utah.edu (H.S. White).

1388-2481/03/$ - see front matter © 2003 Elsevier Science B.V. All rights reserved.
doi:10.1016/S1388-2481(02)00556-8

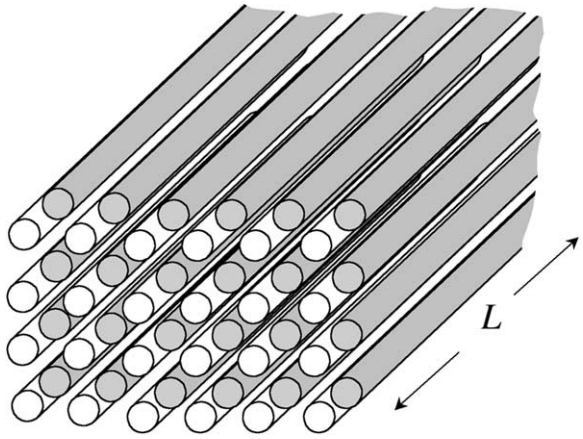

Fig. 1. Schematic diagram illustrating a 3-D microbattery design comprising alternating rows of cylindrically shaped cathodes (grey) and anodes (white). The cathodes and anodes are attached at their bases to flat sheets (not shown) that serve as the current collectors.

current density in a 3-D microbattery is inherently non-uniform – *no 3-D architecture based on the generic cell structure in Fig. 1 will yield a truly uniform primary current distribution*. In general, non-uniform currents result in poor utilization of the electrode materials, and are thus associated with lower cell efficiencies, reduced electrode stability due to non-uniform stresses, and non-uniform heat dissipation [11–13]. The simulations of the current and potential distributions described in this paper provide important insights into future directions for 3-D designs of lithographed or templated electrochemical power sources.

2. Results and discussion

Figs. 2–4 show representative examples of the potential and primary current distributions for representative microbattery designs considered in our investigations. The potential and primary current distributions were computed using both FEHT (F-Chart Software, Middleton, WI) and FiDAP 8.6 software (Fluent USA, Lebanon, NH) and assuming uniform electrolyte conductivity. For simplicity, and to allow comparison of the current densities between different battery designs, all simulations assume identical values of the voltage between cathode and anode. Current

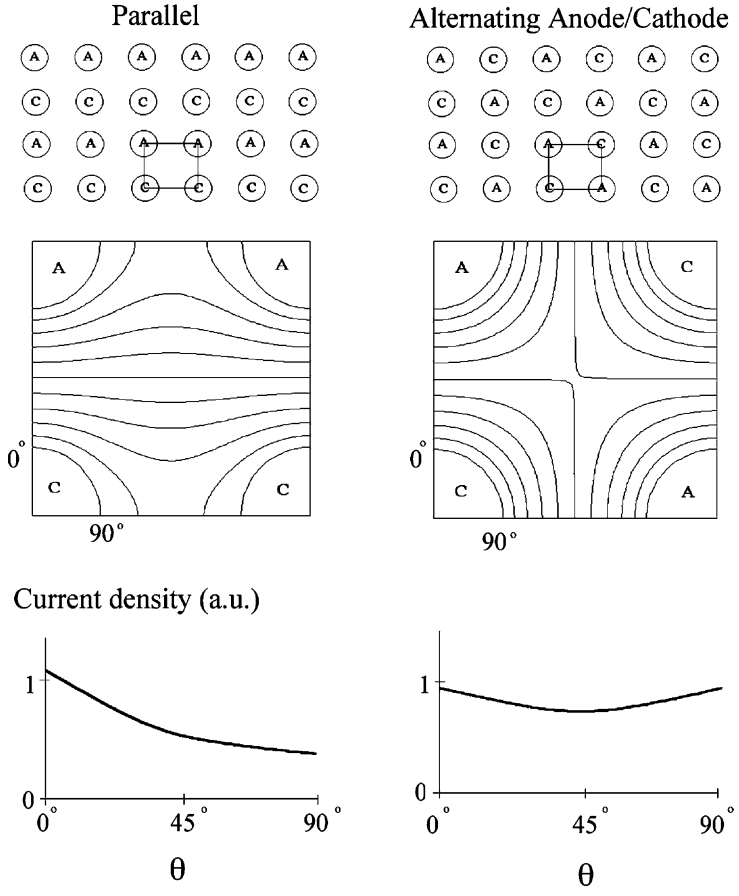

Fig. 2. (Top panels) Schematic diagram of 3-D *cylindrical* battery arrays in *parallel row* (left) and *alternating anode/cathode* (right) configurations. (Middle panels) Isopotential lines between cathode (C) and anode (A) for unit battery cells. (Bottom panel) Current densities (in arbitrary units, a.u.) at the electrode surfaces as a function of the angle θ (see middle panel for definition of θ). The area of the cathodes and anodes are equal throughout the diagram.

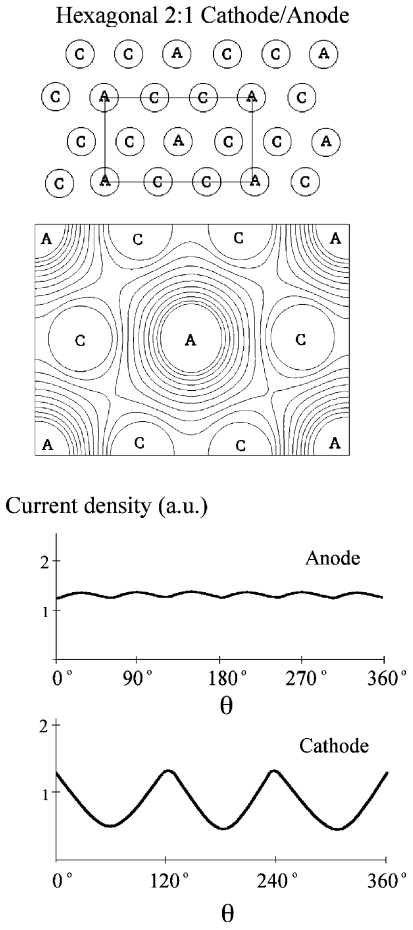

Fig. 3. (Top panel) Schematic diagram of *hexagonal 2:1 cathode/anode* battery array. (Middle panel) Isopotential lines between cathode (C) and anode (A) for unit battery cell. (Bottom panel) Current density at the cathode and anode surfaces, plotted on the same a.u. scale used in Fig. 2.

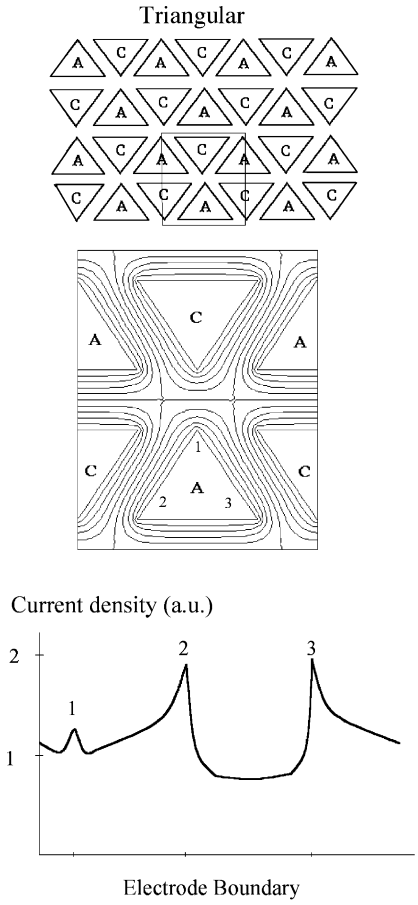

Fig. 4. (Top panel) Schematic diagram of *triangular* battery array. (Middle panel) Isopotential lines between cathode (C) and anode (A) for unit battery cell. (Bottom panel) Current density (a.u.) at the cathode and anode surfaces plotted on the same a.u. scale used in Fig. 2 (see middle panel for the identity of the corner positions).

densities are plotted in the same arbitrary units in each figure, allowing direct comparison of the relative power output of different microbattery geometries. Isopotential lines within the "unit cell" of each microbattery design are also presented. The lengths of the cathodes and anodes, L, are assumed to be equal and sufficiently long to ignore end effects.

Fig. 2 illustrates the sensitivity of the current distribution to electrode placement for two similar microbattery designs. In the *parallel row* design, alternating rows of cylindrically shaped cathodes and anodes are placed on a rectangular grid. This arrangement of electrodes results in high current flow between each neighboring cathode/anode pair (i.e., at $\theta = 0°$), with a relatively steep decrease (~40%) in current between adjacent cathodes or anodes ($\theta = 90°$). A significantly better design based on the rectangular grid is the *alternating cathode/anode* configuration, Fig. 2, in which each anode is surrounded by four nearest-neighbor cathodes (and vice versa). In this geometry, the higher number of nearest-neighbor electrodes of opposite polarity permits a significantly more uniform primary current density at each electrode. However, even in this improved geometry, the current that passes undergoes ~20% fluctuation, a limitation which may not be tolerable in some cells. As expected, current uniformity may be improved by increasing the ratio of the electrode grid spacing to electrode radius in this cell, but at the sake of reducing power density.

It is interesting to consider how energy capacity, active surface area, and other properties of a 3-D battery design, such as the square array shown in Fig. 2, compare to a conventional 2-D thin film design. For the purposes of comparison, we assume a thin film 2-D battery that comprises 1 cm^2-area anode and cathode, each 22.5 μm thick, and separated by a 5-μm thick electrolyte. The total volume of electrodes and separator is 5×10^{-3} cm^3 (the cell housing is ignored for simplicity). It is relatively straightforward to show that a corresponding 3-D square-array battery (Fig. 2) with 5 μm-radius cathode and anodes, a 5 μm-surface-to-surface electrode separa-

tion, and same total volume (i.e., 5×10^{-3} cm^3) contains ~39% of the energy capacity of the thin film design. The lower energy capacity is due to a higher percentage of the total volume being occupied by the electrolyte. On the other hand, the active cathode and anode surface areas in the 3-D design are 3.5 cm^2 each, significantly larger than the 2-D design. However, there are several intriguing advantages of the 3-D design that are not reflected in the above numbers. For instance, the transport length scale in the above thin film 2-D battery is 350% larger than in the 3-D design. Thus, in principle, the 3-D design is significantly less susceptible to ohmic losses and other transport limitations. To achieve equal transport length scales in the 2-D design (i.e., by decreasing the electrode thickness to 5 μm) would require a 330% increase in the areal footprint in order to maintain equal cell volume, a significant disadvantage in employing these devices in MEMS and microelectronic applications. Second, while the above comparison of 2-D and 3-D designs indicates that the 3-D battery has inherently lower energy capacity per total cell volume, in fact, the capacity of the 3-D design can be increased without limit by increasing L, without sacrificing the small areal footprint or high power density. For instance, for the same areal footprint, i.e., 1 cm^2, the above square array 3-D design with $L = 500$ μm has a capacity that is 350% larger than the 2-D design. Such a microbattery would contain 222,222 cathodes and 222,222 anodes, with ~35 cm^2 each of active cathode and anode area! We note that as L is increased, the ohmic resistance of the electrodes will become sufficiently large to offset the advantages of increased capacity. The optimized value of L will be determined by the conductivity of the electrode materials as well as the electrode geometry.

Unlike the conventional battery, a 3-D microbattery need not contain equal number of anodes and cathodes. Indeed, there may be situations where battery design is optimized by using unequal number densities of cathodes and anodes in order to balance the capacities of the active materials and the kinetics of the charge-transfer reactions. Fig. 3 shows an example of a microbattery design utilizing twice as many cathodes as anodes. Here, each anode is surrounded by six cathodes, providing a relatively uniform current density on the anode while sacrificing current uniformity at the cathodes. This design might be useful in a 3-D microbattery where a uniform current density is critical at one electrode (e.g., an insertion electrode).

Finally, as noted above, lithographic fabrication technology allows for the synthesis of essentially any envisioned electrode and cell geometry. Specifically, electrodes need not have a cylindrical shape considered in the previous examples. For example, the closed packed array of triangular-shaped cathodes and anodes shown in Fig. 4 would be expected to yield greater cell capacity and increased power. The trade-off of this design, obviously, is a greatly reduced primary current uniformity. Such a geometry may be appropriate in a situation where the net current is limited by electron-transfer kinetics, and thus the current distribution is uniform across the electrode surface regardless of the electrode geometry.

3. Conclusions

While significant increases in both power and energy density are obtainable from 3-D microbatteries relative to conventional batteries, the inherent difficulty in achieving a uniform current distribution may limit some devices. The several examples presented here demonstrate that there are tremendous opportunities in 3-D microbattery design. Electrode geometries and cell configurations not yet considered are likely to yield current distributions significantly better than the examples described here.

Acknowledgements

This work was supported by the DoD Multidisciplinary University Research Initiative (MURI) program administered by the Office of Naval Research under Grant N00014-01-1-0757 and the Office of Naval Research. FiDAP 8.6 simulations were performed at the University of Utah Center for High Performance Computing.

References

[1] J.D. Joannopoulos, R.D. Meade, J.N. Winn, Photonic Crystals, Princeton University Press, Princeton, NJ, 1995.
[2] See also the special issue on photonic cyrstals, Adv. Mater. 13 (2001) 369.
[3] D.A. Parthenopoulos, P.M. Rentzepis, Science 245 (1989) 843.
[4] S. Sun, C.B. Murray, D. Weller, L. Folks, A. Moser, Science 287 (2000) 1989.
[5] J.H. Holtz, J.S.W. Holtz, C.H. Munro, S.A. Asher, Anal. Chem. 70 (1998) 780.
[6] O.D. Velev, E.W. Kaler, Langmuir 15 (1999) 3693.
[7] E.S. Wu, J.H. Strickler, W.R. Harrell, W.W. Webb, SPIE Proc. 1674 (1992) 776.
[8] B.H. Cumpston, S.P. Ananthavel, S. Barlow, D.L. Dyer, J.E. Ehrlich, L.L. Erskine, A.A. Heikal, S.M. Kuebler, I.-Y.S. Lee, D. McCord-Maughon, J. Qin, H. Rockel, M. Rumi, X.-L. Wu, S.R. Marder, J.W. Perry, Nature 398 (1999) 51.
[9] R.J. Jackman, G.M. Whitesides, Chemtech 29 (5) (1999) 18.
[10] D.H. Gracias, J. Tien, T.L. Breen, C. Hsu, G.M. Whitesides, Science 289 (2000) 1170.
[11] A.C. West, M. Matlosz, D. Landolt, J. Electrochem. Soc. 138 (1991) 728.
[12] M. Orazem, J. Newman, J. Electrochem. Soc. 131 (1984) 2857.
[13] Z. Mao, R.E. White, B. Jay, J. Electrochem. Soc. 138 (1991) 1615.